CrossMark

RESEARCH PAPER

Foam-Filled Grooved Tubes with Circular Cross Section Under Axial Compression: An Experimental Study

Mohammad Mahdi Abedi[1] · **Abbas Niknejad**[1] · **Gholam Hossein Liaghat**[2] ·
Mohammad Zamani Nejad[1]

Abstract In this article, absorbed energy per unit of initial tube length, initial peak force and mean folding force in empty and polyurethane foam-filled simple and grooved specimens with circular cross section are investigated, experimentally. Results demonstrate that in the empty and foam-filled simple specimens, absorbed energy per unit of initial tube length, initial peak force and mean folding force are larger than the corresponding values of the empty and foam-filled grooved specimens, respectively. But, increment of absorbed energy due to the foam-filler in the grooved tubes is more than the corresponding value in the simple specimens. Also, diagrams of absorbed energy and folding force versus the grooves distance have the minimum value. Therefore, there is a critical value for the grooves distance and according to the application viewpoint, to produce a good energy absorber, the grooves distance is selected far from the critical grooves distance. The experimental results show that when the grooves distance (λ) decreases, deformation mode inclines to the concertina (regular) mode and when λ increases, the deformation mode inclines to the diamond mode. Finally, a semiempirical relation is derived to predict the initial peak force of empty and foam-filled grooved tubes.

Keywords Axial compression · Plastic deformation · Folding · Grooved tube · Polyurethane foam

✉ Abbas Niknejad
Aniknejad@yu.ac.ir

1 Mechanical Engineering Department, Yasouj University, P.O. Box 75914-353, Yasouj, Iran

2 Mechanical Engineering Department, Tarbiat Modares University, P.O. Box 14115-143 Tehran, Iran

1 Introduction

Vehicles are mainly designed to satisfy the standards and requirements of general performance, stability, calmness and firm handling. The ability to protect passengers in a car accident depends on the conditions of collision, structural integrity, passenger protective equipment, etc. The front rail in a vehicle chassis acts as the primary defense and bumper to frontal impact during vehicle collision. Therefore, in the design of frontal bumper rails, various thin-walled tubes with circular cross section have largely been used and their deformation behaviors under axial loading have been extensively studied (Kavi et al. 2006; Yang et al. 2007; Ghamarian et al. 2013). Crashworthiness capabilities of five different conjurations of car crash absorbers under quasi-static and dynamic loadings have been investigated, numerically and experimentally (Costas et al. 2013). Liu et al. (2016) investigated the axial dynamic performances of the thin-walled tubes with star-shaped cross sections. They found the specific energy absorption of star-shaped tube is slightly better than that of the polygon tube due to the fact that the deformation mode of star-shaped tube with longer fold length hinders the potential capability of multi-corner tube (Liu et al. 2016). Yin and Wen (2011) studied axial crushing of honeycomb structures with various cell specifications, analytically and numerically. Based on the Super Folding Element theory, they developed a new method for predicting the mean crushing stress of honeycomb structures with various cell specifications under axial loading. Toksoy et al. (2004) found that the use of adhesive can contribute to specific energy absorption of tubes by two mechanisms, namely increased load transfer from tube wall to the foam core and peeling of the adhesive. Guden et al. (2006) investigated interaction coefficients of polystyrene foam-filling of thin-walled aluminum cylindrical tubes

Springer

through compression tests on partially foam-filled tubes with and without adhesive. Experimental load–displacement curves and observation of crushed sections of filled tubes showed that partial foam-filling reduces fold length and hence increases average crushing loads of tubes and proves the interaction effect between tube wall and filler. Mamalis et al. (2003) investigated implementation of the explicit finite element code LS-DYNA to simulate the crush behavior and energy absorption characteristics of thin-walled steel tubes of the same length containing a number of geometrical discontinuities in the form of constant depth grooves. Salehghaffari et al. (2009) investigated the axial crushing behavior of thick-walled tubes with a number of wide grooves, cut from their outer surface, under both static and dynamic loadings. They showed that this design method can significantly control the shaping of axisymmetric folds while the shock absorber crushes axially, and can extend the limits of this most favorable collapsing mode of deformation (Salehghaffari et al. 2009). The influence of longitudinally distributed grooves, deformation mode and energy absorption characteristics of square grooved tubes under axial compression were investigated and compared with that of corresponding simple tubes without grooves (Zhang and Huh 2009). Hosseinipour and Daneshi (2004) studied the axial crushing behavior and crashworthiness characteristics of thin-walled steel tubes containing annular grooves by the experimental method. They demonstrated that the grooves determine positions of folds and control the buckling mode of deformation. They aimed to improve the uniformity of load–displacement behavior and to predict the energy absorption capacity of the tubes (Hosseinipour and Daneshi 2004). The common mechanical features of metallic cellular material under impact loading as well as characterization methods of such behaviors were reviewed by Fang et al. (2010). Mozafari et al. (2015) analyzed effects of foam-filling of aluminum honeycomb core on its in-plane mechanical properties, experimentally and numerically. They found that foam-filling of honeycomb core can increase in-plane crushing strength up to 208 times, and its specific absorbed energy up to 20 times (Mozafari et al. 2015). Flattening process of metal tubes with circular cross section was investigated under lateral compression load between a V-shaped indenter and a platen. Some theoretical formulas were derived to predict the average lateral load, absorbed energy and specific absorbed energy (Niknejad and Tadrisi Javan 2015). Sometimes, the aim of energy, load and deformation mode analyses during the folding or other mechanisms of energy absorption is to achieve a special deformation mode. Therefore, Niknejad et al. (2016a, b) introduced an experimental study on empty and foam-filled thin-walled columns with square and rectangular cross section with centrally circular discontinuities on the longitudinal or latitudinal sides of column cross section

during the local buckling. Baroutaji et al. (2015) presented energy absorption behavior and crashworthiness optimization of short length circular tubes under quasi-static lateral loading. Finite element models were developed using implicit finite element code ANSYS to simulate deformation behavior and energy absorption of circular tubes under lateral loading (Baroutaji et al. 2015). The specific energy absorption of the different tube profiles with different tube thickness and impacting angles was analyzed, and it was found that specific energy absorption increases with increase in tube thickness (Isaac and Oluwole 2016). Niknejad et al. (2015a, b) examined corrugated tubes and found that under lateral loading, a complete corrugated tube with a thicker wall and a smaller diameter is the optimum energy absorber system. Therefore, when a circular tube is transformed into the corrugated tube, a better energy absorber system with a higher capability is achieved under lateral loading, and when the preformed corrugated tubes are filled with polyurethane foam, specific absorbed energy increases by up to 74%. Crashworthiness characteristics of thin-walled steel tubes containing annular grooves were experimentally studied by Hosseinipour and Daneshi (2003). Some theoretical relations were derived to predict diagrams of absorbed energy and axial force versus axial displacement during the folding process in empty and foam-filled quadrangle columns. By considering the folding wavelength as a constant parameter during the folds creation and using balance of internal and external energy and minimum principle in plasticity, final relations were calculated (Abedi et al. 2012; Niknejad et al. 2015a, 2015b). Gradient grooves were preset along thin-walled circular tubes to regulate the collapse process, and the sectionalized theory was developed to predict quadratic upward crushing force (Wei et al. 2016). Darvizeh et al. (2013, 2017) investigated energy absorption characteristics of empty and foam-filled thick-walled grooved tubes under dynamic loading condition by the theoretical and experimental methods. Niknejad et al. (2012, 2016a, b) derived some theoretical relations to predict the mean and instantaneous folding force, total absorbed energy per unit of tube length and specific absorbed energy for polyurethane foam-filled grooved tubes with circular cross section under the axial compression load. During the folding process, a new theoretical model of deformation was introduced for the polyurethane foam-filler.

In the present article, absorbed energy per unit of initial tube length, initial peak force and mean folding force in the empty and polyurethane foam-filled simple and grooved specimens with circular cross section are investigated, experimentally. The effective parameters on their deformation modes are investigated, and a semiempirical relation is derived to predict the initial peak force of empty and foam-filled grooved tubes.

2 Experiments

To investigate energy absorption capacity and the similar parameters, some axial compression tests were carried out on empty and polyurethane foam-filled grooved tubes with circular cross section under the quasi-static loading. Also, some similar tests were performed on the empty and filled tubes with no groove (simple specimen), for better comparison. All the quasi-static tests were carried out with constant loading rate of 5 mm/min. The tubes were made of brass. They were machined, and the circumferential grooves were cut on the inner and outer wall of the tubes, alternatively. In all the specimens, depth of grooves is selected equal to one half of tube wall thickness, and width of grooves is equal to 3 mm.

The first and the last grooves were cut on the inner wall of tubes; therefore, the number of grooves is odd. Total length of the tubes was selected in proportion to the grooves distance. The groove distance indicates half of the folding wavelength (λ), as shown in Fig. 1. Axial compression tests were performed by a universal tension set with commercial brand of DMG (Model 7166). A solid cylindrical specimen of each type of polyurethane foam was prepared, and the quasi-static axial compression tests were carried out. Figure 2 illustrates compressive stress–strain diagram of three types of the polyurethane foam. Material properties of the polyurethane foams were measured and are listed in Table 1. Also, to determine material properties of the tubes, a dumbbell-shaped specimen was prepared according to the standard ASTM E8M and
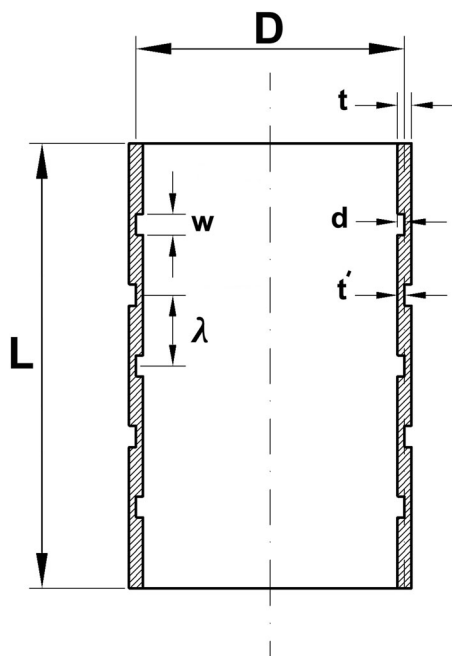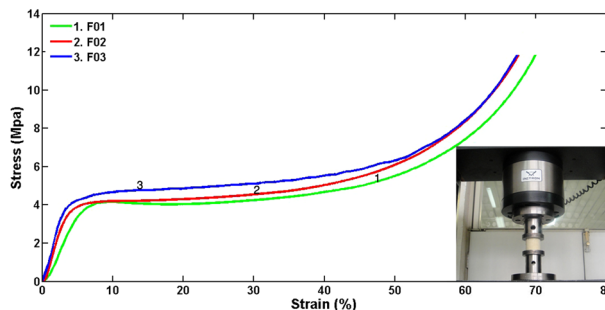

Fig. 2 Compressive stress–strain diagram of the polyurethane foams

Table 1 Material properties of the polyurethane foams

Foam number	Density (kg/m³)	Modulus of elasticity (GPa)	Plateau stress (MPa)
Foam01	222	0.802	4.3
Foam02	244	1.161	4.8
Foam03	260	1.213	5.3

material properties of the tubes were obtained and are listed in Table 2. The axial compression tests were performed on the tubes with different grooves distances and lengths, in both the empty and foam-filled conditions. Tables 3 and 4 give characteristics of the empty and foam-filled specimens, respectively. For each experiment, at least two similar specimens were prepared and tested to affirm repeatability of the experiments. No considerable scatter was observed in the results of the similar samples.

3 Results and Discussion

Figure 3 shows experimental diagram of axial load versus axial displacement during the folds creation in the polyurethane foam-filled grooved specimen F21 with $\lambda = 7$ mm. The corresponding curves of the empty and foam-filled grooved specimens E03 and F05 with $\lambda = 8$ mm are sketched in Fig. 4. Also, Fig. 5 illustrates axial load–displacement diagrams of the empty and filled specimens E11 and F25 with no groove, respectively.

3.1 Effects of Grooves in the Empty and Foam-Filled Specimens

Figure 6 shows experimental load–displacement diagrams of the simple specimen E03 and the grooved specimen E11 with no filler, respectively. Comparison of the curves shows that the grooved creation in the empty circular tube has considerable effects on axial load values. For example, in the simple specimen, the initial force of the first fold creation is larger than the corresponding value of the next folds. On the other

Fig. 1 Characteristics of circular grooved tube

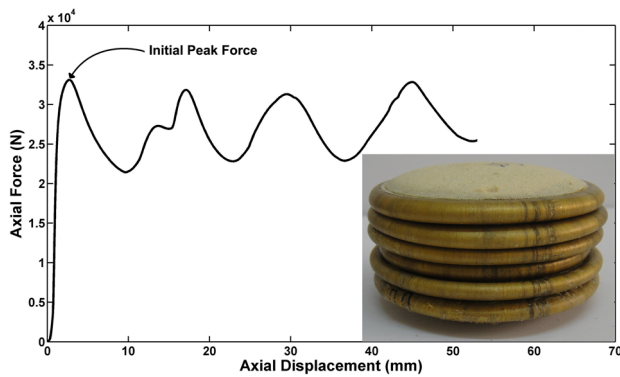**Table 2** Material properties of the simple and grooved tubes

Material type	Density (kg/m^3)	Modulus of elasticity (GPa)	Yield stress (MPa)	Ultimate stress (MPa)	Strain hardening exponent	Flow stress (MPa)
Brass alloy	8700	110	160	376	0.24	220.26

Table 3 Geometrical dimensions of the empty specimens

Empty specimens code	m (g)	L (mm)	D (mm)	t (mm)	t' (mm)	D (mm)	w (mm)	λ (mm)
E01	76.29	36	48.2	1.8	0.9	0.9	3	6
E02	84.99	42	48.2	1.8	0.9	0.9	3	7
E03	93.35	48	48.2	1.8	0.9	0.9	3	8
E04	109.67	54	48.2	1.8	0.9	0.9	3	9
E05	82.30	40	48.2	1.8	0.9	0.9	3	10
E06	91.18	44	48.2	1.8	0.9	0.9	3	11
E07	100.72	48	48.2	1.8	0.9	0.9	3	12
E08	110.01	52	48.2	1.8	0.9	0.9	3	13
E09	127.59	60	48.2	1.8	0.9	0.9	3	15
E10	144.02	68	48.2	1.8	0.9	0.9	3	17
E11	229.62	100	48.2	1.8	–	–	–	–

Table 4 Geometrical dimensions of the foam-filled specimens and type of polyurethane foams-fillers
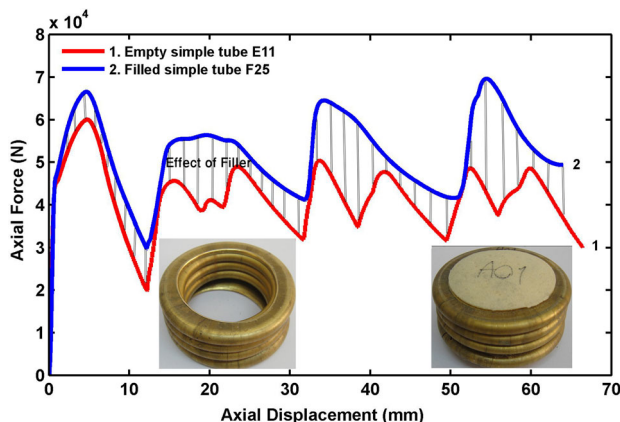
Filled specimens code	Foam-filler type	m (g)	L (mm)	D (mm)	t (mm)	t' (mm)	d (mm)	w (mm)	λ (mm)
F01	Foam01	143.25	60	48.2	1.8	0.9	0.9	3	6
F02	Foam02	142.16	60	48.2	1.8	0.9	0.9	3	6
F03	Foam01	172.35	70	48.2	1.8	0.9	0.9	3	7
F04	Foam02	203.78	84	48.2	1.8	0.9	0.9	3	7
F05	Foam01	162.89	64	48.2	1.8	0.9	0.9	3	8
F06	Foam02	197.88	80	48.2	1.8	0.9	0.9	3	8
F07	Foam01	180.04	72	48.2	1.8	0.9	0.9	3	9
F08	Foam02	221.65	90	48.2	1.8	0.9	0.9	3	9
F09	Foam01	192.23	80	48.2	1.8	0.9	0.9	3	10
F10	Foam02	191.56	80	48.2	1.8	0.9	0.9	3	10
F11	Foam01	220.39	88	48.2	1.8	0.9	0.9	3	11
F12	Foam02	221.06	88	48.2	1.8	0.9	0.9	3	11
F13	Foam01	180.71	72	48.2	1.8	0.9	0.9	3	12
F14	Foam02	177.16	72	48.2	1.8	0.9	0.9	3	12
F15	Foam01	193.39	78	48.2	1.8	0.9	0.9	3	13
F16	Foam02	195.16	78	48.2	1.8	0.9	0.9	3	13
F17	Foam01	151.29	60	48.2	1.8	0.9	0.9	3	15
F18	Foam02	149.92	60	48.2	1.8	0.9	0.9	3	15
F19	Foam01	170.53	68	48.2	1.8	0.9	0.9	3	17
F20	Foam02	170.93	68	48.2	1.8	0.9	0.9	3	17
F21	Foam03	211.79	84	48.2	1.8	1.05	0.75	3	7
F22	Foam03	103.98	40	48.2	1.8	1.05	0.75	3	10
F23	Foam03	138.32	52	48.2	1.8	1.05	0.75	3	13
F24	Foam01	264.87	100	48.2	1.8	–	–	–	–
F25	Foam02	267.94	100	48.2	1.8	–	–	–	–

Fig. 3 Experimental diagram of axial force versus displacement of the filled grooved specimen F21
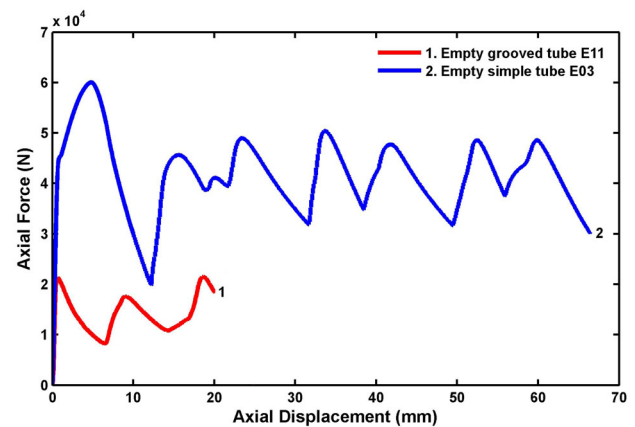

Fig. 4 Experimental diagrams of axial force versus displacement of the grooved specimens E03 and F05

Fig. 5 Experimental diagrams of axial force versus displacement of the simple specimens E11 and F25

Fig. 6 Experimental diagrams of axial force versus displacement of the empty specimens E03 and E11

considerably. It means that although creating the alternative circumferential grooves on the hollow circular tubes reduces the maximum transferred load to the other parts of the structures and its passengers, energy absorption capacity of the initial simple tube is reduced.
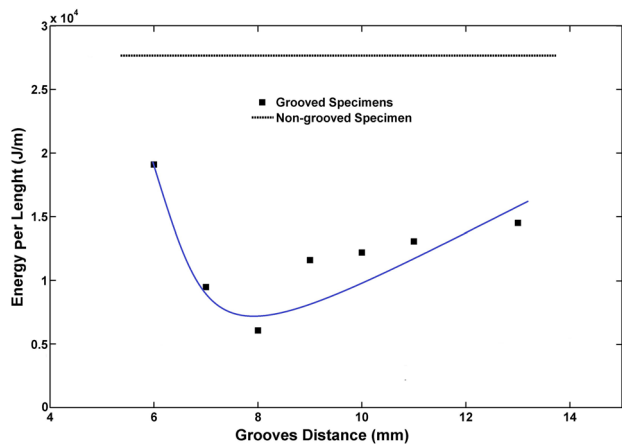
The sketched experimental curve of axial force–displacement of the filled grooved specimen F21 in Fig. 3 illustrates that in the filled grooved specimens, values of peak load of all the formed folds are the same, approximately. In other words, in the filled tubes, by creating the grooves in the tube wall, the first peak load of the first fold creation reduces, and it will be equal to the peak load of the next folds. The curve number 2 in Fig. 4 and the curve number 2 in Fig. 5 illustrate load–displacement diagram of the grooved and simple specimens with polyurethane foam-filler, respectively. Comparison of the graphs ends in the same results as empty specimens. On the other hand, in the filled grooved specimen (F05), axial load peaks of the different folds formation are the same, approximately, but maximum axial load of the first fold creation in the filled simple specimen (F25) is larger than the maximum load during formation of the second and third folds. Therefore, the grooves decrease the maximum force of the first fold in both the empty and filled specimens and it is important in the viewpoint of application. Also, grooves decrease the folding force values over all the deformation.

The experiments show that the number of the formed folds in the empty and filled tubes with circular cross section is controlled by the grooves creation, and the number of folds is equal to the number of the created grooves on the inner wall of the specimens.

3.2 Effects of Grooves Distance in the Empty Specimens

Figure 7 shows experimental measurements of absorbed energy per unit of empty tube length. In the figure, solid

hand, the maximum axial force happens during the first fold formation in the simple circular tube. But, in the empty grooved specimen, all the peaks of folds are almost the same. Also, the figure shows that by machining the circumferential grooves on the inner and outer walls of a circular tube, the initial maximum load and the next relative peaks decrease,

**Fig. 7** Experimental values of the absorbed energy per unit of length versus the grooves distance in empty specimens

squares show experimental results of the empty grooved tubes and the dash-line shows values of absorbed energy/length (E/L) by the similar simple specimen (without groove). The curve-fitted line shows that there is a minimum value for E/L. As shown in the figure, absorbed energy per unit of length by an empty grooved tube firstly decreases, by increasing the grooves distance (λ), and then increases. Therefore, the experiments show that there is a critical grooves distance (λ_{cr}) and the E/L has the minimum value at this point. The critical grooves distance for the present tests is obtained as $\lambda_{cr} = 8$ mm. Hosseinipour and Daneshi (2004) performed some axial compression tests on empty grooved steel tubes. Their research showed that experimental diagram of the absorbed energy per unit of tube length is strictly ascendant versus the grooves distance, but this result contradicts the present article results. This opposition is investigable according to the theoretical viewpoint. Hosseinipour and Daneshi (2003) derived the following relation to predict the absorbed energy by empty grooved tubes per unit of tube length:

$$\frac{E_e}{L} = \frac{\sqrt{3}\pi^2 \sigma_0 D t'^2 + 6\pi\sigma_0\lambda(\lambda t - wd)}{6\lambda} \tag{1}$$

In the above equation, σ_0 is flow stress of the tube material. D and t indicate mean diameter and wall thickness of tubes. d and w are depth and width of grooves, and t' is wall thickness in grooves. The above theoretical relation has a minimum value at critical grooves distance (λ_{cr}); therefore, the experimental results of the present article have a correlation with the theoretical predictions, but the presented experimental results by Hosseinipour and Daneshi (2004) do not agree with their suggested theory (Hosseinipour and Daneshi 2003). Although the derived relation (Eq. 1) by Hosseinipour and Daneshi (2003) and the performed experiments in the present articles show a critical value for the grooves distance, the values are not the same; this
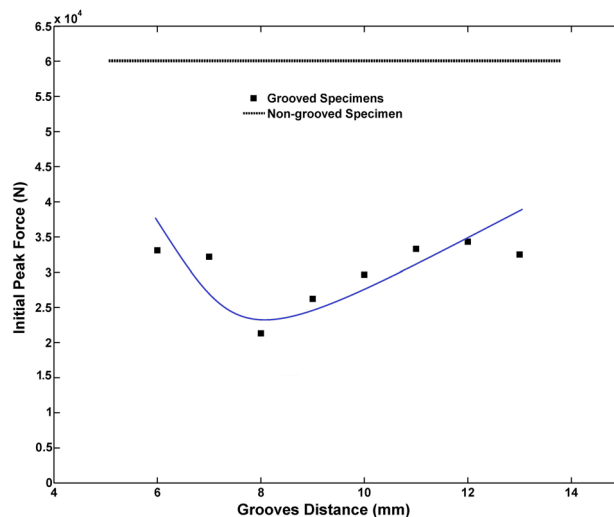
Fig. 8 Experimental values of the initial peak force versus the grooves distance in empty specimens
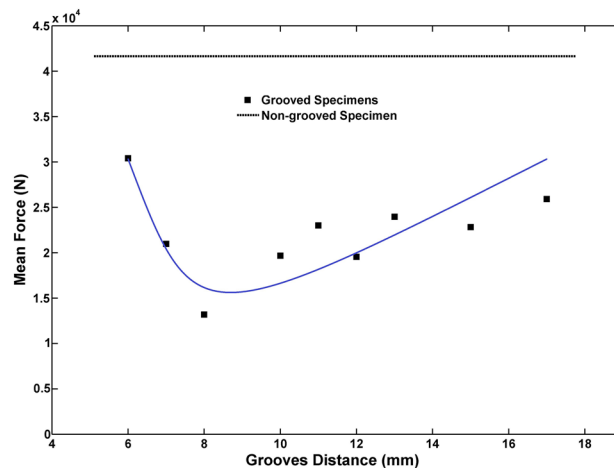

Fig. 9 Experimental values of the mean folding force versus the grooves distance in empty specimens

means that the theoretical analysis (Hosseinipour and Daneshi 2003) needs further consideration and modifications.

Figures 8 and 9 show initial peak force (P_i) and mean folding force (P_m) of the empty tubes versus the grooves distance, respectively. The figures show that the parameters E/L, P_i and P_m have a minimum value at the critical grooves distance, according to the experiments. The critical grooves distance for all the mentioned parameters is the same and equal to $\lambda_{cr} = 8$ mm. Niknejad et al. (2012) suggested the following relation to predict the mean folding force of a empty grooved tube during the axial compression:

$$P_m = \frac{\sqrt{3}\pi^2 \sigma_0 D t'^2 + 6\pi\sigma_0\lambda(\lambda t - wd)}{3(1.72\lambda - t)} \tag{2}$$
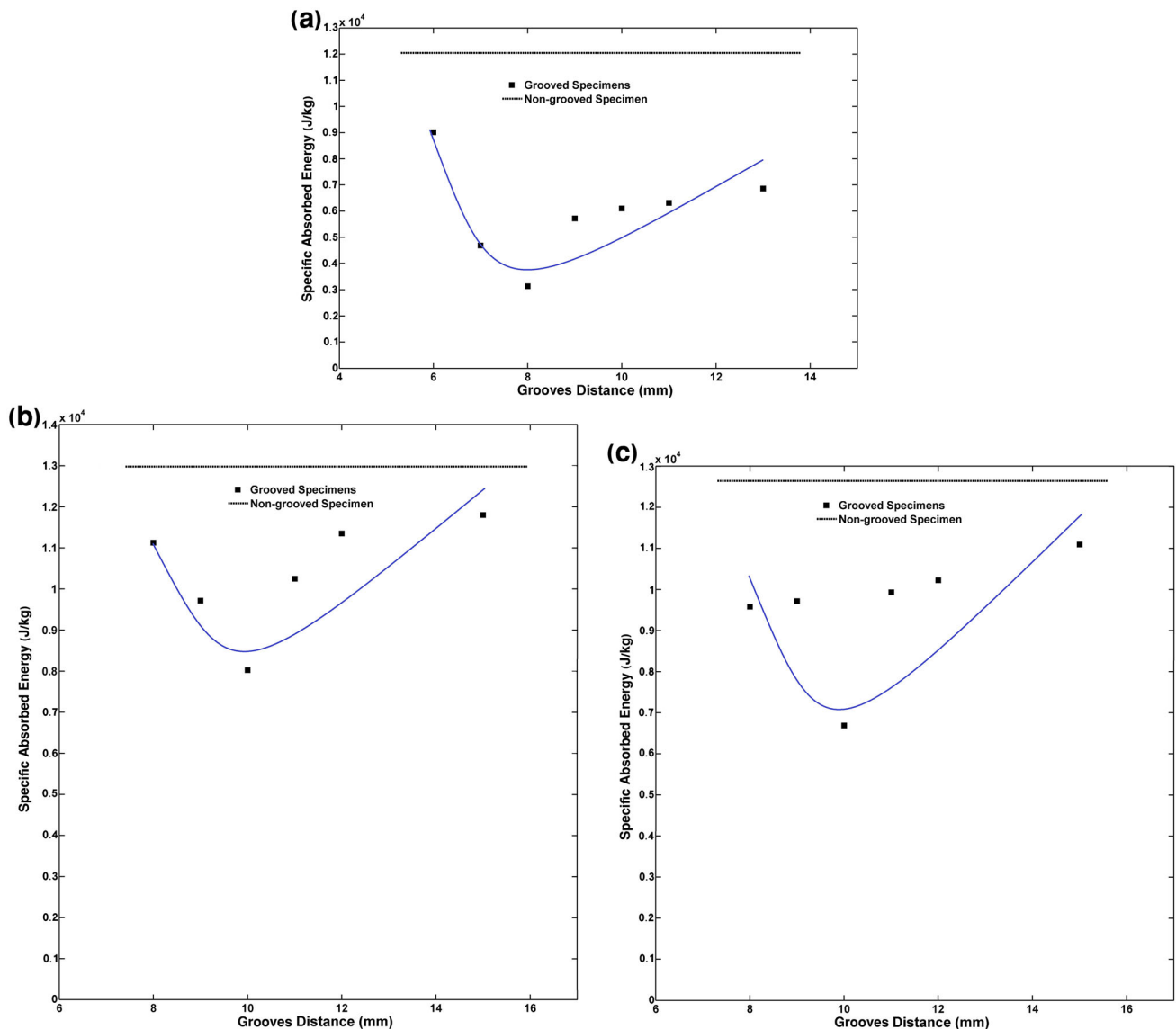
Fig. 10 Experimental values of the specific absorbed energy versus the grooves distance in **a** empty specimens, **b** filled specimens with the foam-filler Foam01 and **c** filled specimens with the foam-filler Foam02

The above relation has a minimum value; therefore, the experimental results of this article in contrast with the presented experimental results by Hosseinipour and Daneshi (2003) agree with the previous theoretical analyses. The derived relation (Eq. 2) by Niknejad et al. (2012) and the performed experiments in the present article shows a critical value for the grooves distance; however, the values are not the same. Therefore, the theoretical analysis (Niknejad et al. 2012) needs more consideration and modifications.

Figure 10a illustrates specific absorbed energy (absorbed energy per mass) by the empty specimens during the folding process. The figure shows that the empty grooved tubes have the specific absorbed energy between 3500 and 8500 J/kg. Also, the figure demonstrates that in

the empty grooved tubes, critical grooves distance is equal to 8 mm and when the grooves distance is selected higher than or less than the mentioned critical value, specific absorbed energy increases.

3.3 Effects of Grooves Distance in the Filled Specimens

Figures 11, 12 and 13 show the experimental diagram of absorbed energy/length, initial peak point ($P_{i,f}$) and mean folding force ($P_{m,f}$) of the foam-filled grooved tubes, based on the axial compression tests. Figure 11 shows experimental results of the specimens with the foam-filler of Foam01, and Figs. 12 and 13 illustrate the experimental
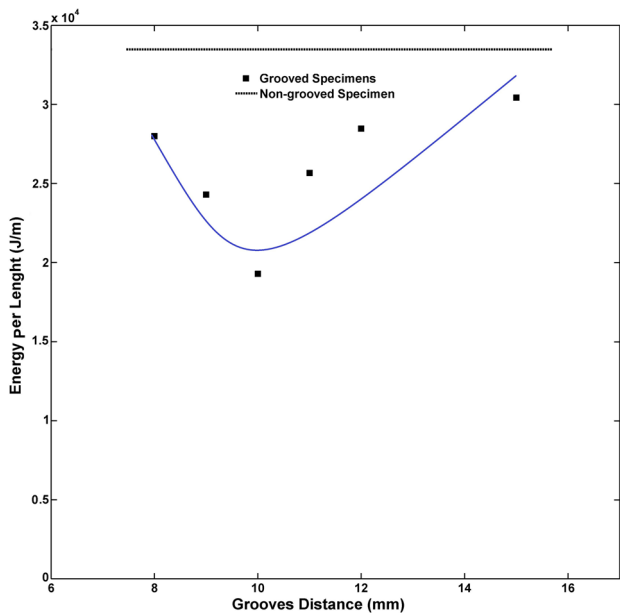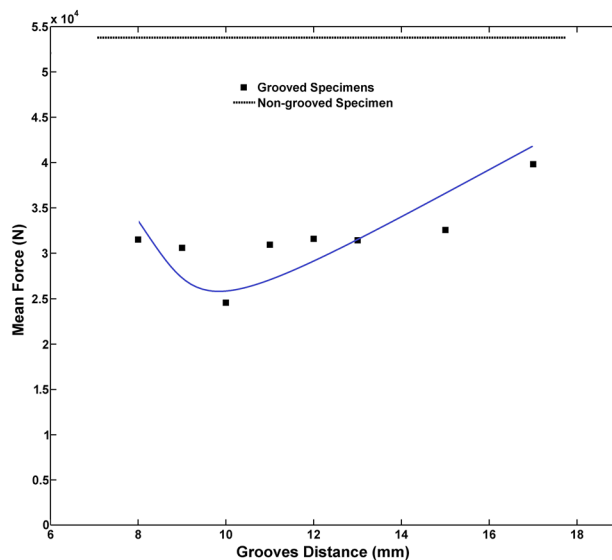
Fig. 11 Experimental values of the absorbed energy per unit of length versus the grooves distance in foam-filled specimens with the foam-filler Foam01
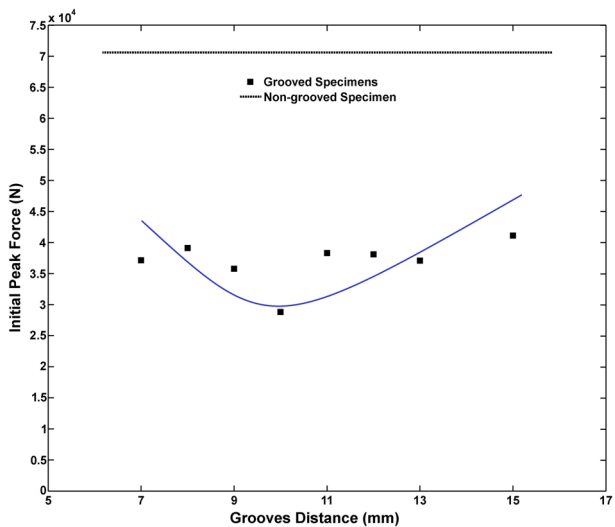
Fig. 12 Experimental values of the initial peak force versus the grooves distance in foam-filled specimens with the foam-filler Foam02

measurements of the specimens with the foam-filler of Foam02. In all the figures, E/L, $P_{i,f}$ and $P_{m,f}$ have a minimum value at the critical grooves distance. Therefore, there is a critical value for the grooves distance and according to the application viewpoint, to produce a good energy absorber, the grooves distance is selected far from the λ_{cr}. The critical grooves distance is obtained as $\lambda_{cr} = 10$ mm.

Niknejad et al. (2012) derived the following theoretical relation for estimating the absorbed energy by a foam-filled grooved tube per unit of tube length:

Fig. 13 Experimental values of the mean folding force versus the grooves distance in foam-filled specimens with the foam-filler Foam02

$$\frac{E_{tot}}{L} = \frac{\sqrt{3}}{6\lambda}\pi^2\sigma_0 Dt'^2 + \pi\sigma_0(\lambda t - wd) + \frac{0.25\pi\sigma_p}{\lambda}[4Ddw + (D - t)^2(1.72\lambda - t)]$$
(3)

In the above relation, σ_p indicates plateau stress of the polyurethane foam. Equation (3) has a minimum value at the critical grooves distance. Therefore, in design of an energy absorber from the foam-filled grooved specimens, the grooves distance must be selected far from the λ_{cr} to gain a high energy absorption capacity. Table 5 shows the experimental and theoretical values of E/L in the foam-filled specimens. As given in Table 5 and based on this viewpoint, error percentages show that the experimental results have an acceptable agreement with the previous theoretical relation.

Also, Fig. 11 shows that energy absorption/length of the filled grooved tubes is less than the E/L of the corresponding filled simple tube (without groove) and it can be assumed that a simple specimen is a grooved specimen with infinity grooves distance. As shown in Fig. 7, the same result is obtained for the empty specimens.

Figure 14 shows the relationship of E/L of the foam-filled grooved specimens to E/L of the empty grooved specimens versus the grooves distance. Also, the horizontal line shows the corresponding ratio for the simple specimens. The figure shows that increment of absorbed energy due to the foam-filler in the grooved tubes is more than the increment of absorbed energy in the simple specimens. On the other hand, the polyurethane foam-filler has more effect on energy absorption capacity for the grooved tubes, compared to the simple specimens.

Table 5 Experimental and theoretical values of absorbed energy per unit of length in the foam-filled specimens
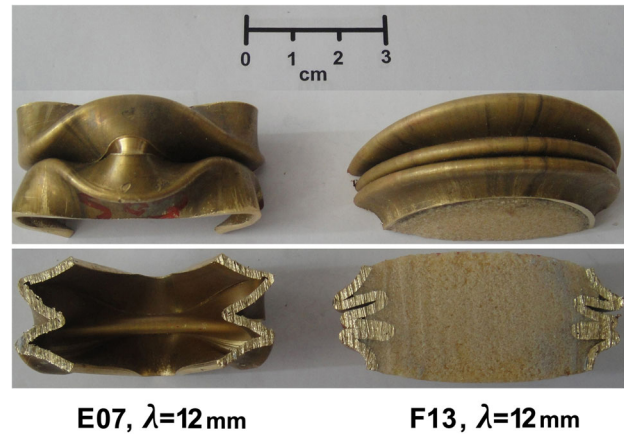
| Filled specimens code	Absorbed energy per unit of length (J/m)		Difference percentage
	Experiments	Equation (3)	
F01	19,636	20,306	3.41
F02	21,463	21,541	0.36
F03	23,615	21,238	10.07
F04	20,792	22,504	8.23
F05	28,000	22,248	20.54
F06	24,000	23,538	1.92
F07	24,291	23,311	4.03
F08	23,929	24,619	2.88
F09	19,283	24,410	26.59
F11	25,666	25,536	0.51
F12	24,150	26,871	11.26
F13	28,476	27,843	2.22
F14	25,158	31,565	25.46
F17	30,430	30,199	0.76
F21	25,268	23,770	5.93
F22	29,988	27,055	9.78
F23	32,902	30,549	7.15
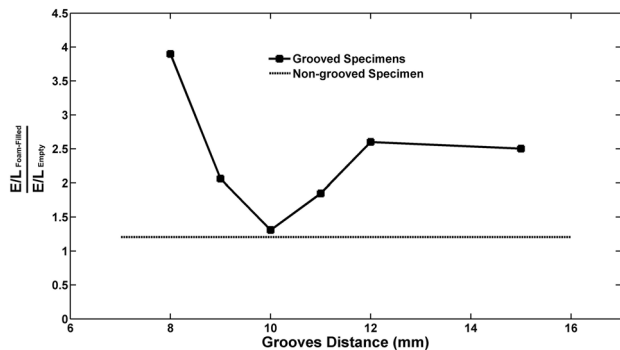
Fig. 14 Ratio of E/L of the filled (Foam02) grooved specimens to E/L of the empty grooved specimens versus the grooves distance

Fig. 15 Deformation modes of the foam-filled grooved specimen F13 and empty grooved specimen E07 with the same grooves distance
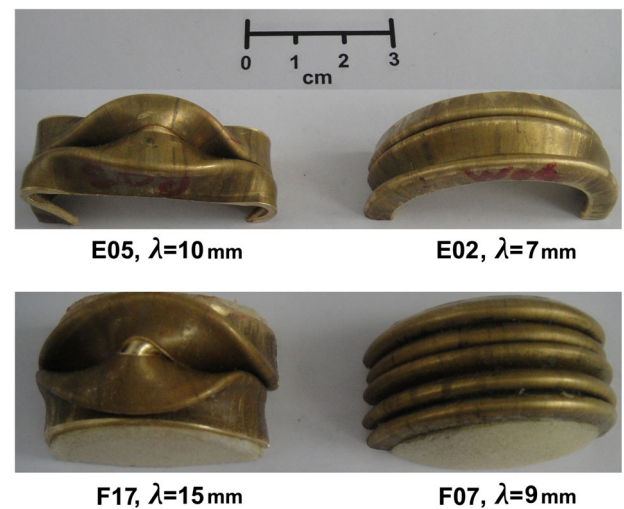
Fig. 16 Deformation modes of the foam-filled and empty grooved specimens with different grooves distances

Figure 10b and c shows specific absorbed energy by the filled specimens with the foam-fillers of Foam01 and Foam02, respectively. As shown in the figure, it is found that the filled grooved tubes by the fillers of Foam01 and Foam02 have the specific absorbed energy between 64,000 and 12,000 J/kg. Also, the figure shows that in the filled grooved tubes, critical grooves distance is equal to 10 mm, and when the grooves distance is selected higher than or less than the mentioned critical value, specific absorbed energy increases.

Figure 15 compares deformation modes of the foam-filled grooved specimen F13 and the empty grooved specimen E07 with similar grooved distance of $\lambda = 12$ mm. The figure shows that the foam-filler changes the deformation mode from diamond to concertina. The created folds in the filled specimen are more regular than the formed folds in the empty specimen.

Figure 16 compares deformation modes of two empty and two filled specimens with different grooves distances. The figure shows that there are two different modes of deformation in the grooves specimens: diamond and concertina. The experimental results show that when the grooves distance decreases, the deformation mode inclines to the concertina (regular) mode and when λ increases, the deformation mode inclines to the diamond mode. Therefore, it is concluded that change in the grooves distance causes change in the deformation mode. Also, it is demonstrated that in both the empty and foam-filled grooves tubes, when λ decreases, more regular deformation occurs in the specimens.

Fig. 17 Deformation modes of the foam-filled grooved specimen F19 and F20 and empty grooved specimen E10 with the same grooves distance

E10, λ=17mm   **F19, λ=17mm**   **F20, λ=17mm**

Generally, in both the grooved tubes and the simple tubes, 2λ is equal to the folding wavelength. Therefore, in the grooved tubes, λ indicates the grooves distance or half of the folding wavelength. Experimental observations on the empty samples show that when a simple tube is axially compressed, the tube is folded with an intrinsic folding wavelength, but when a grooved tube with a certain grooves distance of λ is axially compressed, the grooved tube is folded with a folding wavelength equal to 2λ. In the folding process on the empty grooved tubes, when the grooves distance of a tube is larger than half of the intrinsic folding wavelength of the corresponding initial simple tube, the grooved specimen is folded in the diamond mode; and when the grooves distance of the tube is less than half of the intrinsic folding wavelength of the corresponding initial simple tube, the grooved specimen is folded in the concertina mode. Also, experimental observations on the foam-filled samples show that when the grooves distance is less than a certain value, the filled grooved tube is folded in the concertina mode and when the grooves distance increases and is selected larger than the certain value, deformation mode changes to the diamond mode. However, due to the compressive resistance of the internal foam-filler, in the filled grooved condition, diamond mode occurs in the specimens with longer grooves distance, compared to the corresponding empty grooved tubes.

To complete the recent discussion, Fig. 17 illustrates deformation modes of the specimens E10, F19 and F20 after the axial compression process. The specimen E10 has been tested in the empty condition, but the specimens F19 and F20 have been compressed in the filled condition by the fillers of Foam01 and Foam02, respectively. All the specimens have the same grooves distance of 17 mm. The figure shows that the empty specimen E10 has been compressed in the diamond mode, and it is due to its larger grooves distance, with respect to half the intrinsic folding wavelength of the corresponding empty simple tube. Furthermore, the figure demonstrates that the filled specimen F19 with the foam-filler of Foam01 has been folded in the

diamond mode, while the filled specimen F20 with the foam-filler of F20 has been compressed in the concertina mode. Plateau stress of Foam02 is higher than the corresponding value of Foam01. Therefore, as shown in Fig. 17, it is found that both the foam-filler strength and grooves distance have considerable effects on deformation mode of the grooved tubes during the axial compression tests. In other words, in the polyurethane foam-filled grooved tubes, when grooves distance is higher than a certain value, if plateau stress of the foam-filler is less than a critical value, the filled tube is compressed in the diamond mode; if plateau stress of the filler is higher than the critical value, the filled tube is folded in the concertina mode.

3.4 Prediction of the Initial Peak Force

Mean folding force of an empty grooved tube was derived by Niknejad et al. (2012) as the theoretical relation (2). Initial peak point of load–displacement diagram indicates the minimum required load for forming the folds in grooved specimens. This point is illustrated in Fig. 3, for a filled specimen. Based on the experimental measurements on the empty grooved specimens, initial peak load of an empty circular tube is considered proportional to the mean folding force. Therefore,

$$P_i = kP_m = \frac{\sqrt{3}\pi^2\sigma_0 Dt'^2 + 6\pi\sigma_0\lambda(\lambda t - wd)}{3(1.72\lambda - t)} \cdot k \qquad (4)$$

Figure 18 illustrates experimental values of the coefficient k versus the grooves distance in the empty grooved specimens. In this figure, calculated values for the coefficient k were obtained by substituting the geometrical characteristics of the empty specimens in the right side of the above equation and the corresponding experimental values of the initial peak load P_i in the left side of Eq. (4). The figure shows that the semiempirical mean value of k is equal to 1.64. Therefore, the following relation is obtained to predict the initial peak load of an empty grooved tube during the axial compression:
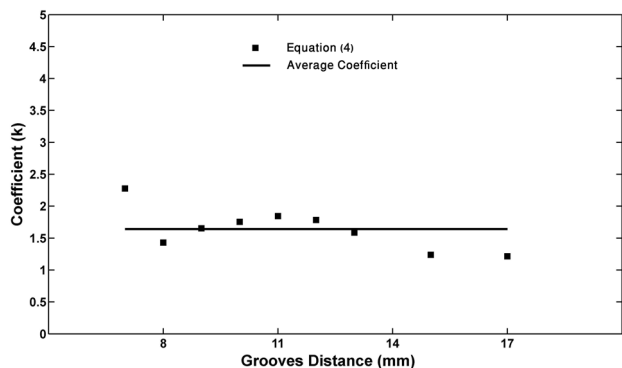
Fig. 18 Experimental value of the coefficient k for different empty grooved tubes versus the grooves distance

Table 6 Experimental and theoretical values of initial peak force in the empty specimens

Empty specimens code	Initial peak force (N)		Difference percentage
	Experiments	Equation (5)	
E02	32,180	23,192	27.93
E03	21,320	24,466	14.75
E04	26,220	26,016	0.78
E05	29,660	27,751	6.44
E06	33,300	29,614	11.07
E07	34,320	31,570	8.01
E08	32,500	33,596	3.37
E09	28,520	37,798	32.53
E10	31,220	42,137	34.96

$$P_i = \frac{2.84\pi^2\sigma_0 Dt'^2 + 9.84\pi\sigma_0\lambda(\lambda t - wd)}{3(1.72\lambda - t)} \quad (5)$$

Table 6 gives experimental values of initial peak loads and the corresponding theoretical calculations by Eq. (5) and difference percentages.

In the next stage, value of initial peak of load–displacement diagram of the polyurethane foam-filled grooved tubes is considered as shown below:

$$P_{i,f} = P_i + P_f \quad (6)$$

where P_f and $P_{i,f}$ indicate axial compression force of the polyurethane foam and axial folding force of the foam-

Table 7 Experimental and theoretical values of initial peak force in the foam-filled specimens

| Empty specimens code	Filled specimens code Experiments	Initial peak force (N) Equation (8)
F01	34,465	30,705
F02	36,018	30,183
F03	36,426	31,496
F04	37,134	30,977
F05	44,941	32,742
F06	39,108	32,224
F07	42,345	34,272
F08	35,781	33,756
F09	33,640	35,990
F10	28,820	35,475
F11	39,300	37,840
F12	38,300	37,326
F13	42,380	39,786
F14	38,100	39,272
F15	37,740	41,803
F16	37,080	41,290
F17	40,860	45,991
F18	41,120	45,479
F19	38,040	50,320
F20	36,200	49,809
F21	33,138	35,854
F22	42,768	39,370
F23	48,349	44,696

filled grooved tubes, respectively. The axial compression load of the polyurethane foam, with the initial volume equal to the internal volume of the grooved tube, was calculated as the following (Niknejad et al. 2012):

$$P_f = \frac{\pi\sigma_p[4Ddw + (D-t)^2(1.72\lambda - t)]}{4(1.72\lambda - t)} \quad (7)$$

Substituting Eqs. (5) and (7) into (6) results in:

$$P_{i,f} = \frac{2.84\pi^2\sigma_0 Dt'^2 + 9.84\pi\sigma_0\lambda(\lambda t - wd) + 0.75\pi\sigma_p[4Ddw + (D-t)^2(1.72\lambda - t)]}{3(1.72\lambda - t)} \quad (8)$$

The above relation predicts initial peak load of the polyurethane foam-filled specimens during the folding process under the axial loading. Table 7 gives experimental measurements of initial peak force of the filled grooved specimens and the corresponding predictions by Eq. (8). Error percentage of the theoretical predictions is illustrated in Fig. 19. The figure shows that between the 23 filled

Springer

Fig. 19 Error percentage of theoretical predictions of initial peak force in foam-filled grooved tubes
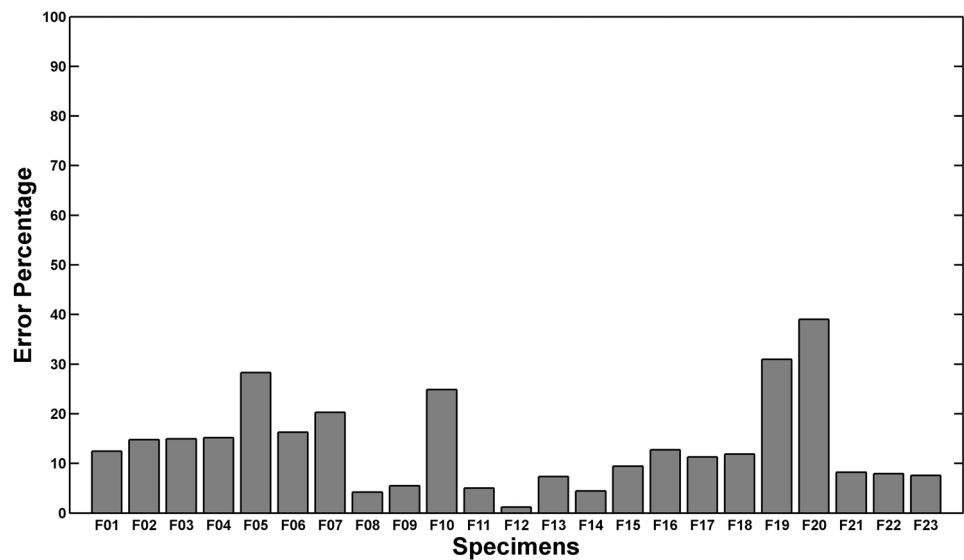
specimens, error percentage of 10 specimens is less than 10% and error percentage of the theoretical predictions for 18 specimens is less than 20%.

In designing the chassis frames of vehicles to withstand impact in the event of an accident, energy absorption characteristics of critical components of the frames must be analyzed. Thus, increasing the specific absorbed energy by structures and especially thin-walled structures has been one of interesting and practical subjects, and foam-filling of thin-walled structures is one way to improve the safety of frontal bumper rails, the present article suggests using thin-walled grooved tubes as an energy absorber system with a high crashworthiness performance in the design of frontal bumper rails of automobiles to increase the vehicle safety.

4 Conclusion

This article studies the axial compression of simple and grooved specimens with circular cross section in two different conditions: empty and polyurethane foam-filled by the experimental method. It is concluded that the grooves decrease the maximum force of the first fold in both the empty and filled specimens, and it is important in viewpoint of application because this phenomenon reduces transitional force to the other parts of structure and its passengers that are in series with the grooved energy absorber. Also, grooves decrease folding force values over all the deformation. Consequently, foam-filler is used to compensate the reduction in energy level due to the grooves creation. The experiments show that the number of the formed folds in the empty and filled tubes with circular cross section is controlled by the grooves creation, and number of the folds is equal to the number of the created

grooves on the inner wall of the specimens. One of the most important advantages of using the grooved tubes as an energy absorber is eliminating or enhancing the limitation of maximum length of the used tube under the axial compression. On the other hand, due to occurrence of the stress concentration in the grooves, the tube tends to local buckling (folding process) instead of global buckling.

Effects of the grooves distance on total energy absorption per unit of tube length, initial peak force and mean folding force of the empty and foam-filled grooved tubes were investigated, and it was found that all diagrams of the mentioned quantities in the empty and foam-filled grooved specimens versus grooves distance have a minimum value. Therefore, the corresponding value of the grooves distance in the minimum point was introduced as critical grooves distance and for producing a good energy absorber, the grooves distance must be selected far from the λ_{cr}.

The polyurethane foam-filler has more effects on energy absorption by the grooved specimens, compared to the simple specimens. Finally, some semiempirical relations were introduced to predict initial peak point in the force–displacement diagrams of the empty and foam-filled grooved tubes, which shows a good correlation with the experimental measurements.

Although the performed investigations and comparisons show that the semiempirical relations, developed for estimating the initial peak load of the empty and filled grooved tubes, have acceptable accuracy, and error percentages of about 75% of specimens are less than 15%, some of them have more error. Thus, the present article invites other researchers to perform their future works in this field with the main purpose of increasing the accuracy of the theoretical relations.

References

Abedi MM, Niknejad A, Liaghat GH, Zamani Nejad M (2012) Theoretical and experimental study on empty and foam-filled columns with square and rectangular cross section under axial compression. Int J Mech Sci 65:134–146

Baroutaji A, Gilchrist MD, Smyth D, Olabi AG (2015) Crush analysis and multi-objective optimization design for circular tube under quasi-static lateral loading. Thin Walled Struct 86:121–131

Costas M, Diaz J, Romera LE, Hernandez S, Tielas A (2013) Static and dynamic axial crushing analysis of car frontal impact hybrid absorbers. Int J Impact Eng 62:166–181

Darvizeh A, Darvizeh M, Ansari R, Meshkinzar A (2013) Effect of low density, low strength polyurethane foam on the energy absorption characteristics of circumferentially grooved thick-walled circular tubes. Thin Walled Struct 71:81–90

Darvizeh A, Meshkinzar A, Alitavoli M, Rajabiehfard R (2017) Low velocity impact of empty and foam filled circumferentially grooved thick-walled circular tubes. Thin Walled Struct 110:97–105

Fang DN, Li YL, Zhao H (2010) On the behaviour characterization of metallic cellular materials under impact loading. Acta Mech Sin 26:837–846

Ghamarian A, Zarei HR, Farsi MA, Ariaeifar N (2013) Experimental and numerical crashworthiness investigation of the empty and foam-filled conical tube with shallow spherical caps. Strain 49:199–211

Guden M, Toksoy AK, Kavi H (2006) Experimental investigation of interaction effects in foam-filled thin-walled aluminum tubes. J Mater Sci 41:6417–6424

Hosseinipour SJ, Daneshi GH (2003) Energy absorption and mean crushing load of thin-walled grooved tubes under axial compression. Thin Walled Struct 41:31–46

Hosseinipour SJ, Daneshi GH (2004) Experimental studies on thin-walled grooved tubes under axial compression. Exp Mech 44:101–108

Isaac WC, Oluwole O (2016) Energy absorption improvement of circular tubes with externally press-fitted ring around tube surface subjected under axial and oblique impact loading. Thin Walled Struct 109:352–366

Kavi H, Toksoy AK, Guden M (2006) Predicting energy absorption in a foam-filled thin-walled aluminum tube based on experimentally determined strengthening coefficient. Mater Des 27:263–269

Liu W, Lin Z, Wang N, Deng X (2016) Dynamic performances of thin-walled tubes with star-shaped cross section under axial impact. Thin Walled Struct 100:25–37

Mamalis AG, Manolakos DE, Ioannidis MB, Kostazos PK, Kastanias SN (2003) Numerical modelling of the axial plastic collapse of externally grooved steel thin-walled tubes. Int J Crashworthiness 8:583–590

Mozafari H, Molatefi H, Crupi V, Epasto G, Guglielmino E (2015) In plane compressive response and crushing of foam filled aluminum honeycombs. J Compos Mater 49(26):3215–3228

Niknejad A, Tadrisi Javan Y (2015) Circular metal tubes during lateral compression between a V-shape indenter and a platen—theory and experiment. Proc IMechE Part L J Mater Des Appl 229(4):318–331

Niknejad A, Abedi MM, Liaghat GH, Zamani Nejad M (2012) Prediction of the mean folding force during the axial compression in foam-filled grooved tubes by theoretical analysis. Mater Des 37:141–151

Niknejad A, Abedi MM, Liaghat GH, Zamani Nejad M (2015a) Absorbed energy by foam-filled quadrangle tubes during the crushing process by considering the interaction effects. Arch Civ Mech Eng 15:376–391

Niknejad A, Abdolzadeh Y, Rouzegar J, Abbasi M (2015b) Experimental study on the energy absorption capability of circular corrugated tubes under lateral loading and axial loading. Proc IMechE Part D J Automob Eng 229(13):1739–1761

Niknejad A, Abedi MM, Liaghat GH, Zamani Nejad M (2016a) Foam-filled grooved tubes with circular cross-section under axial compression: a theoretical analysis. Iran J Sci Technol Trans Mech Eng 40:155–167

Niknejad A, Firouzi M, Saadatfard H (2016b) Experimental investigations on the folding process of polyurethane foam-filled aluminium columns with circular discontinuities. Iran J Sci Technol Trans Mech Eng 40:359–367

Salehghaffari S, Tajdari M, Mokhtarnezhad F (2009) The collapse of thick-walled metal tubes with wide external grooves as controllable energy-dissipating devices. Proc IMechE Part C J Mech Eng Sci 223(11):2465–2480

Toksoy AK, Tanoglu M, Guden M, Hall IW (2004) Effect of adhesive on the strengthening of aluminum foam-filled circular tubes. J Mater Sci 39:1503–1506

Wei Y, Yang Z, Yan H, Guo Y, Wu X, Huang C (2016) Proactive regulation of axial crushing behavior of thin-walled circular tube by gradient grooves. Int J Mech Sci 108–109:49–60

Yang IY, Lee KS, Park SG, Cha CS (2007) The axial collapse characteristics of hat shaped section members in a vehicle. J Mater Proc Technol 187–188:136–139

Yin H, Wen G (2011) Theoretical prediction and numerical simulation of honeycomb structures with various cell specifications under axial loading. Int J Mech Mater Des 7:253–263

Zhang X, Huh H (2009) Energy absorption of longitudinally grooved square tubes under axial compression. Thin Walled Struct 47:1469–1477